

THE THERMAL RESPONSE OF GENERIC OBJECTS IN JP-4 POOL FIRES

by

J.T. Nakos, W. Gill and N.R. Keltner

Thermal Test & Analysis Division 7537
Sandia National Laboratories
Albuquerque, N.M., 87185

ABSTRACT

The measured thermal response of generic objects in engulfing pool fires is presented. The objects include cylinders and flat plates of various sizes and materials. A simple radiation/convection model of the heat transfer from the fire to the object is developed and discussed in light of the experimental data.

INTRODUCTION

The purpose of this paper is to first describe the Sandia National Laboratories fire testing capabilities for simulating severe transportation accidents, then present details of acquiring data and predicting the heat transfer to generic objects and finally to discuss the limitations of the heat transfer model. The utility of the heat transfer model would be in its post-test predictive capability in the analysis of actual fire data.

Sandia National Laboratories maintains fire test facilities for subjecting a variety of test items to the so called abnormal accident environment. A typical test involves exposing the test item to an engulfing pool fire for a time period of 30 to 60 minutes. Items normally tested at the facility include hazardous materials shipping containers, weapon components, and conventional ordnance.

FACILITY DESCRIPTIONS

The tests have been run in open pools; a 9 m x 18 m (30 x 60 ft) concrete lined pool, a 1.8 m x 5.5 m (6 x 18 ft) stainless steel pool and a 3.0 m (10 ft) diameter steel tub. Also available is a 6.1 m x 6.1 m (20 ft x 20 ft) square steel "bund" that sets down in the concrete pool.

The above pools are all "open pools" that allow natural air flow into the fire. There are also two other facilities at the site that are enclosed and have forced air flow into the combustion chamber. These facilities are specifically designed to simulate the thermal environment in an open pool fire while providing an afterburner to burn out the soot in the plume. The smallest facility, called the SWISH (Small WInd SHielded) facility is fitted with a 1.8 m (6 ft) diameter pool which is housed in a 5.5 m (18ft) high spray water cooled structure. A larger facility, called SMERF (SMoKe Emission Reduction Facility), is being brought on line. This facility has a 3.0 m x 3.0 m (10 ft x 10 ft) square pool and uses water filled walls for cooling.

All of the facilities can be connected to a Hewlett-Packard data acquisition system (DAS) capable of sampling 120 type K thermocouple channels and 20 "high level" (0-5v) voltage channels. In addition, a smaller DAS is available, and can sample up to 60 more channels.

Over the past several years an effort has been made to include in the fires some type of generic object, such as a cylinder or a plate, and record its thermal response. The information from these experiments has been used to build an extensive data base from which several thermal models have been developed, one of which is discussed herein. These models have been used to characterize the fire environment, predict the response of generic objects, and allow an analytical approach in the design of fire resistant items.

EXPERIMENTAL DEVICES AND DATA ACQUIRED

Experimental data have been gathered on a small stainless steel cylindrical calorimeter (SSSCC), two flat plate calorimeters (FPC's), a large mild steel cylindrical calorimeter (LMSCC) and several pool flux calorimeters (PFC's). All of these calorimeters are basically a steel plate or cylinder with one side facing the fire and the other side insulated; the insulated side having a thermocouple mounted on its surface. The cylindrical calorimeters are normally oriented with the cylinder centerline horizontal, the FPC is mounted with the plates vertical, and the pool flux calorimeters are mounted with the outer surface facing upward, into the fire.

On the fire side all the calorimeters are instrumented with 1.6 mm (1/16") diameter, ungrounded junction, inconel sheathed, type K (chromel-alumel) thermocouples. These thermocouples were called flame thermocouples and are mounted just off the outer surface in the fire, some with a thin steel radiation shield placed between the thermocouple and the surface. The FPC's had shielded fire thermocouples, the SSSCC, LMSSC and PFC did not have shields.

The inner surface temperature measurements from the calorimeters are used as inputs to a computer code which solves the inverse heat conduction problem and calculates the total absorbed heat flux through the outer calorimeter surface versus time as well as the outer surface temperature versus time. This information along with the thermocouple measurements taken from just off the calorimeter surface have been used to develop a heat transfer model.

Transpiration radiometers were flush mounted on the outer surface of the FPC's. Transpiration radiometers are devices that measure only the radiative component of the heat flux; the convective part being eliminated from the measurement, see [1]. However, transpiration radiometers are expensive to fabricate and difficult to use, and so their data are not always available.

In what follows, the details of acquiring and reducing the heat flux data are presented. A heat transfer model is also developed and discussed.

EXPERIMENTS AND PROCEDURES

CALORIMETER DESCRIPTIONS

The SSSCC is a 22.2 cm (8.75") outside diameter x 30.5 cm (12") long x 2.2 cm (7/8") thick cylinder made of 304 stainless steel. Four, 1.6 mm (1/16") diameter, type K, ungrounded junction, sheathed thermocouples were mounted on the inside wall of the cylinder, spaced every 90°. The entire space inside the cylinder was packed with high temperature insulation and the ends were covered with steel plates. Four other sheathed thermocouples were mounted 5.1 cm (2") off the outer surface of the calorimeter, at the same axial and circumferential location as the inside thermocouples. Figure 1 shows a sketch of the SSSCC.

The FPC's are made of a heavily instrumented pair of vertically oriented flat steel plates. The plates on both FPC's are about 30.5 cm (12") wide and 305 cm (10 ft) long. They are mounted side by side. An FPC used in the first test series (TRUPACT II tests) had one 0.5 cm (3/16") thick 304 stainless steel plate and a 1.9 cm (3/4") thick mild steel plate. The FPC used in the second test series (On-Site Container test) had 2 mild steel plates, one 3.18 cm (1.25") thick and the other 3.81 cm (1.50") thick.

Thermocouples were mounted on the inner surface of the plates and about 10 cm (4") off the surface of the plates to measure the flame temperature. In addition, there were transpiration radiometers mounted on the outer surface of the plates to measure the radiative component of the heat flux.

Figures 2 and 3 show an overall view and a sectional view of the plate calorimeter used in the TRUPACT-II testing. The major differences between the two FPC's were the plate materials and thicknesses and the number of heavily instrumented stations. The On-Site FPC had both plates made of thick mild steel and two heavily instrumented measurement stations, one at 2.5 ft and the other at 7.5 ft from the leading edge. The TRUPACT-II FPC had a mild steel and stainless steel plate and only one heavily instrumented measurement station, at 2.5 ft from the leading edge.

Figure 4 shows a side view of the LMSSC. The LMSSC is made of A517 mild steel, is 1.4 m (56") diameter and 6.4 m (21 ft) long. The wall is 3.2 cm (1.25") thick and has reinforcing ribs every 61 cm (24") along the length. Measurements included flame temperatures and temperatures on the inner surface of the 3.2 cm thick walls.

Figure 5 shows a cut-away view of a typical pool flux calorimeter. The sensing element is a 0.64 cm (0.25") thick, 7.62 cm (3") diameter mild steel disk. A thermocouple is mounted on the inner surface, which is also heavily insulated. Analyses have shown that as the fuel surface recedes, the heat transfer remains essentially one dimensional.

POOL LAYOUTS

The layout of the 1.8 m x 5.5 m (6 ft x 18 ft) pool is shown in Figure 6, in plan view. This pool is used for tests

where only one side of the test item is to be exposed to the fire. The test unit is mounted outside the pool, directly over the long edge. The three instrumentation towers were located 45.7 cm (18") from the pool edge. Flame thermocouples (on all 3 towers) and calorimeters (on 2 towers) were used to measure the temperature and heat flux. The flame thermocouples were at 1.2, 1.8, 2.4, 3.0 and 3.7 m (4, 6, 8, 10, 12 ft) from the pool floor and the calorimeters were at 2.4 m from the floor.

The layout of the 9 m x 18 m (30 ft x 60 ft) pool is shown in Figure 7. The long axis of the pool is oriented in the east-west direction. The test unit, a shipping container, was located on the east side and the 1.4 m diameter calorimeter was located on the west side. The long axis of the test unit was oriented east-west while the long axis of the 1.4 m calorimeter was oriented north-south. The FPC was placed between the test unit and the LMSCC, north of the centerline of the pool. The transpiration gages in the FPC faced south, into the fire. As indicated in Figure 7, there were other experiments in the pool, but those results will not be presented here. The pool was filled with water 61 cm (24") deep and JP-4 fuel to a depth of about 20 cm (8"). This amounted to about 33,000 liters (8,800 gal) of fuel.

TESTS PERFORMED

The data that will be presented came from several tests performed in the pools described above. The tests performed in the 1.8 m x 5.5 m (6 ft x 18 ft) pool were of a section of the Safe Secure Transport (SST) trailer. There were 3 tests, two "calibration" tests to define the setup and one test with an SST wall section. The 3 tests were between 35-40 minutes long.

The data from the 9 m x 18 m (30 ft x 60 ft) pool came from two tests. Three tests of the TRUPACT-II shipping container were performed, each about 30-36 minutes long. Data from only the first test will be presented here. Other data came from a test of a hazardous material shipping container. That test was about 17 minutes long.

ANALYSIS

ENERGY BALANCE & HEAT TRANSFER MODEL

Calculation of the thermal response of an object in a fire begins with an energy balance on the outer surface:

$$q_{\text{net}} = q_{\text{ir}} - q_{\text{er}} + q_{\text{c}} - q_{\text{refl}}, \quad (1)$$

where q_{net} is the net absorbed heat flux, q_{ir} the incident radiant flux, q_{er} the emitted radiative flux, q_{c} the convective heat flux, and q_{refl} is the reflected radiative flux. Note that condensation of any kind is neglected in this model. Equation (1) may be simplified by noticing that $q_{\text{ir}} - q_{\text{refl}} = q_{\text{a}}$, where q_{a} is the absorbed radiative flux $\alpha_{\text{s}}q_{\text{ir}}$:

$$q_{\text{net}} = \alpha_{\text{s}}q_{\text{ir}} + h_{\text{s}}(T_{\text{f}} - T_{\text{s}}) - \varepsilon_{\text{s}}\sigma(T_{\text{s}}^4 - T_{\infty}^4). \quad (2)$$

T_{s} is the surface temperature of the object, T_{f} is the flame temperature, α_{s} and ε_{s} are the surface absorptivity and emissivity, σ is Stefan-Boltzmann constant and h_{s} is the convective film coefficient. Equation (2) can be expanded by assuming Fourier's Law for heat conduction in the solid wall:

$$-k(T)(\partial T(x,t)/\partial x) = h_{\text{s}}(t)(T_{\text{f}}(t) - T_{\text{s}}(t)) + \alpha_{\text{s}}q_{\text{ir}}(t) - \varepsilon_{\text{s}}(T)\sigma(T_{\text{s}}(t)^4 - T_{\infty}(t)^4), \quad (3)$$

where the thermal conductivity k , specific heat c and surface emissivity ε_{s} are properties of the calorimeter wall and can be temperature dependent. Little error results from assuming that the environment temperature $T_{\infty}(t)=0$, i.e. that the environment is cold compared to the fire.

A computer code SODDIT (Sandia One Dimensional Direct and Inverse Thermal) [2] in its direct mode uses equation (3) and calculates the temperature in the calorimeter wall as a function of time given $q_{\text{ir}}(t)$. The radiation flux q_{ir} is calculated from the relation:

$$q_{\text{ir}} = \varepsilon_{\text{f}}\sigma T_{\text{f}}^4, \quad (4)$$

where ε_{f} is the flame emissivity, and T_{f} is the "flame temperature" as measured by the thermocouple just off the calorimeter surface. ε_{f} varies with the flame thickness L and an extinction coefficient κ .

Average values for the flame emissivity determined from transpiration gage data were 0.82 and 0.75 from two different tests. These values were obtained by comparing average heat flux values from the transpiration gages with average flux values calculated from equation (4). The flame emissivity ϵ_f was varied until the averages agreed. Another way to estimate ϵ_f is to use the relation

$$\epsilon_f = 1 - e^{-\kappa L}, \quad (5)$$

where $\kappa \approx 1 \text{ m}^{-1}$ for JP-4 pool fires from [3]. The flame thickness L can be estimated from the size of the fire and the placement of the calorimeter.

A value for h_g of $56.8 \text{ W/m}^2\text{-}^\circ\text{C}$ ($10 \text{ Btu/ft}^2\text{-hr-}^\circ\text{F}$) has been found to give good agreement with experimental data during the fire. This value also agrees with the experimental value given in Russell and Canfield [4], i.e., $56.1 \text{ W/m}^2\text{-}^\circ\text{C}$ ($9.88 \text{ Btu/ft}^2\text{-hr-}^\circ\text{F}$). After the fire the value $h_g=11.4 \text{ W/m}^2\text{-}^\circ\text{C}$ ($2 \text{ Btu/ft}^2\text{-hr-}^\circ\text{F}$) was used to represent free convective heat transfer.

The key assumption in this model is that the single thermocouple reading the "flame" temperature can be used in two places. First, it is used as the flame temperature in the incident radiative heat flux term, equation (4). Second, it is used as the fluid temperature in the convection term, equation (2) or (3). This assumption is probably in error; it is unlikely that the measured temperature is exactly both the fluid and the flame temperature. However, if it is close to them both, it can be used to model the thermal response of the object in a relatively easy manner using, equation (3). As the results will show, the agreement using the single thermocouple measurement is generally good when the thermocouples are shielded.

RESULTS

The validity of the heat transport model is investigated by using the SODDIT code in the inverse mode. In its inverse mode, the code uses the measured temperature on the inside wall of the calorimeter to calculate the $q_{ir}(t)$ and the exposed fire side surface temperature. The outer surface temperature estimated by SODDIT is called a "measured" value, because it has been shown to agree quite well with actual measured temperatures [5]. This measured surface temperature is then compared with the surface

temperature calculated (called "predicted") from SODDIT in the direct mode.

DATA FROM THE SSSC

Figures 8-11 show results from the SSSCC. The data are from the SST (Safe Secure Transport) trailer wall section test series. They show experimental and predicted temperature data from the bottom and north sides of the SSSCC. The data is from the surface of the calorimeter that faces the fire. Figure 8 shows data from the bottom, with and without convection. The results assume a flame thickness of 2.4 m (8 ft, the height above the pool). Using the extinction coefficient of $\kappa=1\text{m}^{-1}$, the flame emissivity from equation (5) is 0.91. The value used for the convective heat transfer coefficient during the fire, $h_g=56.8\text{ W/m}^2\text{-}^\circ\text{C}$ (10 Btu/ft²-hr-°F), came from work to be reported in Brown, et.al., [6] and from Russell and Canfield [4] for JP-5 fires. The value $h_g=11.4\text{ W/m}^2\text{-}^\circ\text{C}$ (2 Btu/ft²-hr-°F) after the fire is a free convective value believed to be representative of the post fire situation. As can be seen, the agreement between the measured and predicted results with convection is within 15% at the maximum temperatures seen.

Figure 8 also shows the predicted temperature without convection, i.e., $h_g=0$. As can be seen, the predicted response is further below the actual response and below the predicted response with convection, except towards the end of the fire. This implies that on a small cylinder, convection can play an important role in the total heat transfer early in the fire, when the temperature difference between the calorimeter and the fire is large.

Figure 9 shows data from the north side of the calorimeter, closest to the wall, in the first "calibration" test. Because the north side faced a hot wall for most of the test, the flame thickness was assumed large and so the flame emissivity was set to 1.0. The same convection heat transfer coefficients were used as before. The results with convection agree to within 10% at the maximum temperatures, and are close during the rise. However, without convection, the results are much worse early in the fire, and the difference at the maximum temperatures is up to 15%. This again implies that convection plays an important role in the total heat transfer early in the fire.

Figures 10 and 11 show results from the first test of the SST wall panel. The winds were very low and the fire

very intense, therefore, the calorimeter temperature rose to over 1100 C (2000 F) on the north side. As can be seen from the figures, agreement between the measured and predicted temperatures is quite good.

DATA FROM THE FPC

Figures 12-13 show results from the FPC during the TRUPACT-II test series, test 1. In this test the flame emissivity was estimated from transpiration gage data. The average value of the radiative flux was compared with the average value predicted from the shielded flame thermocouple using varying values for the flame emissivity, ϵ_f . For TRUPACT-II, test 1, ϵ_f was found to be 0.82. A similar calculation in the hazardous material container test 1 gave $\epsilon_f=0.75$. Note that the flame temperature thermocouples on both FPC's were shielded.

Figure 12 shows the data on the mild steel side, with and without convection. As can be seen, the predicted results are much closer to the actual temperatures with convection. The predicted results with convection and the actual temperatures agree to within about 5% at the highest temperatures seen.

The results in Figure 13, on the stainless steel side, also show good agreement (8%). Only the results with convection are presented.

Figures 14-17 show data from hazardous material container test #1. The plate calorimeter used in these tests was slightly different than that used in the TRUPACT-II test series, as described earlier. The flame emissivity was estimated from transpiration gage data and found to be 0.75. $h_g=56.8 \text{ W/m}^2\text{-}^\circ\text{C}$ (10 Btu/ft²-hr-°F) during the fire and $h_g=11.4 \text{ W/m}^2\text{-}^\circ\text{C}$ (2 Btu/ft²-hr-°F) after the fire, as before. Note that the transpiration gage used to estimate ϵ_f was at the lower station of the plate calorimeter, and so the results should be best at the lower station.

Figures 14 and 15 show data from the lower station, and the agreement is very good. Figures 16 and 17 show data from the upper station, located 7.5 ft from the leading edge. Although still good, the agreement between the predicted and measured results is not as good as that at the lower station, and in fact the predicted results are actually higher than the actual results. This usually does not occur, i.e., the predicted results are usually lower than the actual

temperatures. This overprediction probably occurs because of an overestimation of the flame emissivity at the upper station, which causes a higher than actual heat flux in the thermal model.

DATA FROM THE LMSCC

Data from the LMSCC can be viewed in Figures 18 & 19. This calorimeter is a thermally massive object in the fire and will actually affect the fire in such a way that the amount of heat flux reaching the calorimeter is less than with a smaller object. This phenomenon has been observed experimentally [7] and then predicted analytically [6], [8]. Remember that the flame temperature thermocouples in this situation were not shielded.

The results show good agreement between predicted and actual temperatures for both the bottom and top of the calorimeter. The predicted surface temperature is too high on the bottom but the agreement is very good on the top. The good agreement is somewhat surprising because one would expect that the thermocouple, which is not shielded and is close to a large cold surface, would read below the actual radiation flame temperature. Fry [9] and Keltner, et.al. [10], showed that up to a 30% error in the thermocouple reading could occur under certain situations similar to the one near the LSMCC. However, the thermocouple, mounted approximately 10 cm (4") from the surface, appears to read close to the effective radiation temperature of the flux reaching the surface, and therefore the good agreement results.

One should note that there is a steep temperature gradient close to the LMSCC. This cooler layer of combustion products reduces the heat flux to the surface, see [6], [8] and [11]. This is called "radiation blocking" or the "thermal mass effect".

POOL FLUX CALORIMETERS

An example showing the limitations of the model can be seen in Figure 20. Figure 20 shows the predicted and actual response of a pool flux calorimeter during the hazardous material container test #1. As can be seen, the agreement is not very good. An unshielded thermocouple was used to monitor the flame temperature about 5.1 cm (2") above the calorimeter face. This thermocouple "saw" the fuel surface at perhaps 150 C (300 F) and the fire above at

about 800 C (1475 F). This configuration probably generates a considerable error in flame temperature, see [10]. Because the flame temperature is raised to the 4th power to obtain heat flux, a (for example) 20% error in temperature generates an 80% (approx) error in heat flux.

DISCUSSION

The information from these experiments has been used to build an extensive data base from which a simple thermal model has been developed. This model has been used to predict the response of generic objects, and allow an analytical approach in the design of fire resistant items.

1) A simple thermal model has been developed that is flexible and relatively easy to use.

2) With only temperature dependent material properties and a "flame" temperature measurement, a good prediction ($\pm 15\%$ or better at the maximum temperature) of the actual thermal response of several generic objects in pool fires was obtained.

3) With the temperature boundary condition at the outer surface known, designers could conceivably predict the response of the internal parts of their "object". This could be especially useful when a post-mortem of an object in an actual test shows unexpected results.

4) Measurements from shielded thermocouples seemed to generate the most accurate predictions.

ACKNOWLEDGEMENTS

The authors would like to thank L.A. Kent, W.R. Jacoby, J.T. Meloche, and B.G. Strait for their support in the fabrication, data acquisition and data reduction of the work presented in this paper. Sandia National Laboratories is operated by AT&T Technologies for the U.S. Department of Energy (DOE) under Contract DEAC0476DP00789.

NOMENCLATURE

h = convective heat transfer coefficient, W/m^2-C
 q = heat flux, kW/m^2
 T = temperature, C
 ϵ = emissivity
 σ = Stefan-Boltzman const., $5.6693 \times 10^{-12} W/cm^2-K^4$

α = absorptivity

Subscripts

c = convective heat flux
er = emitted radiative heat flux
f = flame temperature value
ir = incident radiative heat flux
net = net flux to surface
refl = reflected heat flux
s = surface

REFERENCES

- [1] Matthews, L., Longenbaugh, R., and Mata, R., "Transpiration Radiometer in Fire Characterization", InTech, ISA, August, 1986.
- [2] Blackwell, B.F., Douglass, R.W., Wolf, H., "A Users Manual for the Sandia One-Dimensional Direct and Inverse Thermal (SODDIT) Code", SAND85-2478, May, 1987.
- [3] Longenbaugh, R.S., and Matthews, L.K., "Experimental and Theoretical Analysis of the Radiative Transfer Within a Sooty Pool Fire", Sandia National Laboratories, Report SAND86-0083, Albuquerque, New Mexico, February, 1988.
- [4] Russell, L.H., Canfield, J.A., "Experimental Measurement of Heat Transfer to a Cylinder Immersed in a Large Aviation-Fuel Fire", J. Heat Transfer, August, 1973, pp 397-404.
- [5] Nakos, J.T. and Keltner, N.R., "The Radiative-Convective Partitioning of Heat Transfer to Structures in Large Pool Fires", Heat Transfer Phenomena in Radiation, Combustion and Fires, ASME-HTD, Vol. 106, Book No. H00498 - 1989.
- [6] Brown, N.N., Nicolette, V.F., Bainbridge, B.L., Keltner, N.R., Nakos, J.T., and Sobolik, K.B., "Fire Boundary Condition Studies", Sandia National Laboratories, Report SAND89-2432, TTC-0945, Albuquerque, NM, June 1990.
- [7] Gregory, J.J., Keltner, N.R., and Mata, R., Jr., "Thermal Measurements in Large Pool Fires", Heat and Mass Transfer in Fires, ASME-HTD-VOL. 73, pp 27-36, 1987.
- [8] Nicolette, V.F., and Larson, D.W., "The Influence of Large, Cold Objects on Engulfing Fire Environments", to be presented at the AIAA/ASME Thermophysics and Heat Transfer Conference, Seattle, WA., June, 1990.

[9] Fry, C.J., "A Consideration of Some Simple Models for Assessing Heat Transfer to Objects Engulfed in Pool Fires", AEE Winfrith, AEEW-M 2321, Winfrith, GB, March, 1985.

[10] Keltner, N.R., Sobolik, K.B., and Moya, J.L., "Heat Transfer in Severe Accident Simulations", Presented at the 9th International Symposium on the Packaging and Transportation of Radioactive Materials, June 11-16, 1989, Washington, D.C.

[11] Keltner, N.R., Nicolette, V.F., Brown, N.N., and Bainbridge, B.L., "Test Unit Effects on Heat Transfer in Large Fires", To be presented at the 2nd International Specialist Meeting on Major Hazards in the Transport and Storage of Pressure Liquified Gases, Queen's University, Kingston Ontario, Canada, May 27-30, 1990.

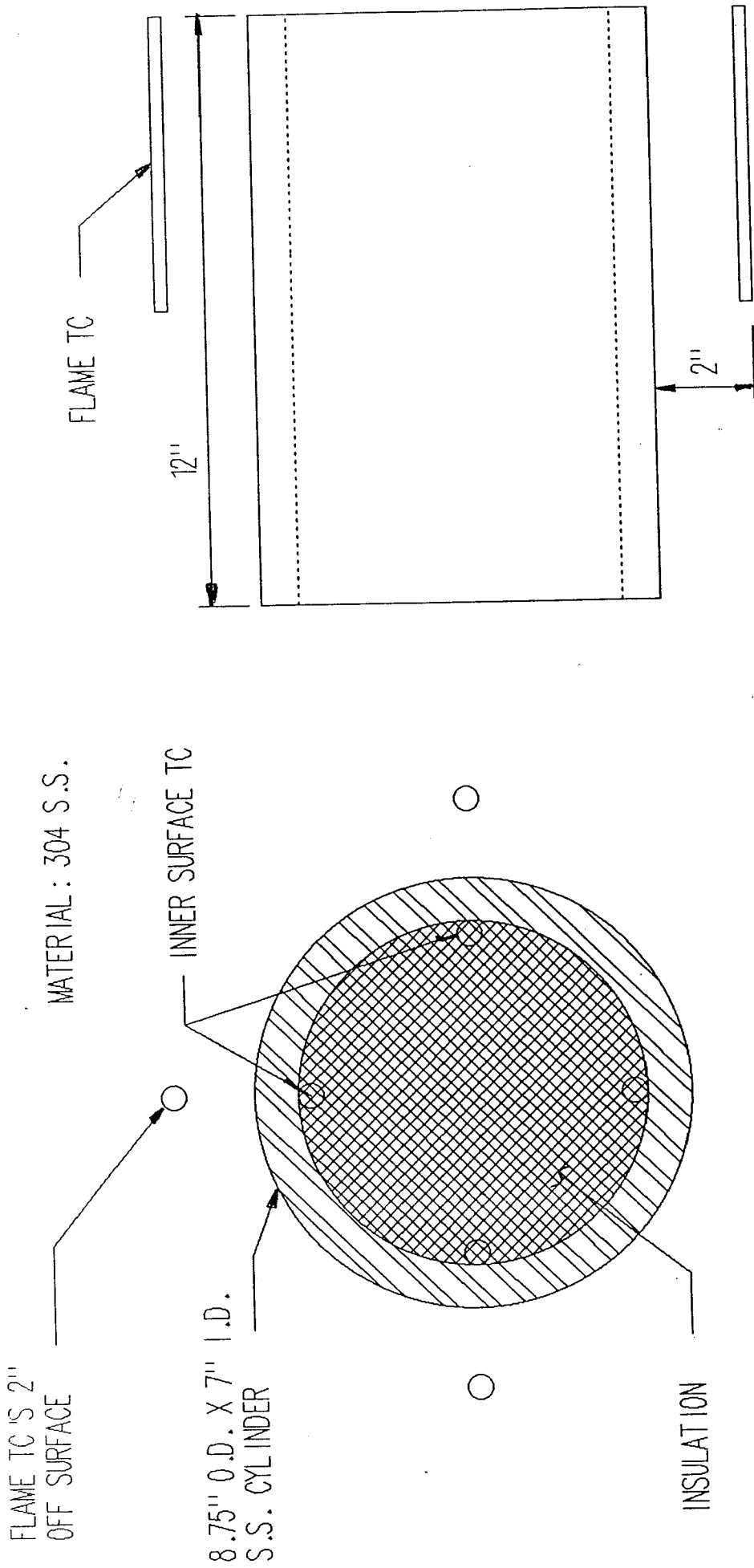
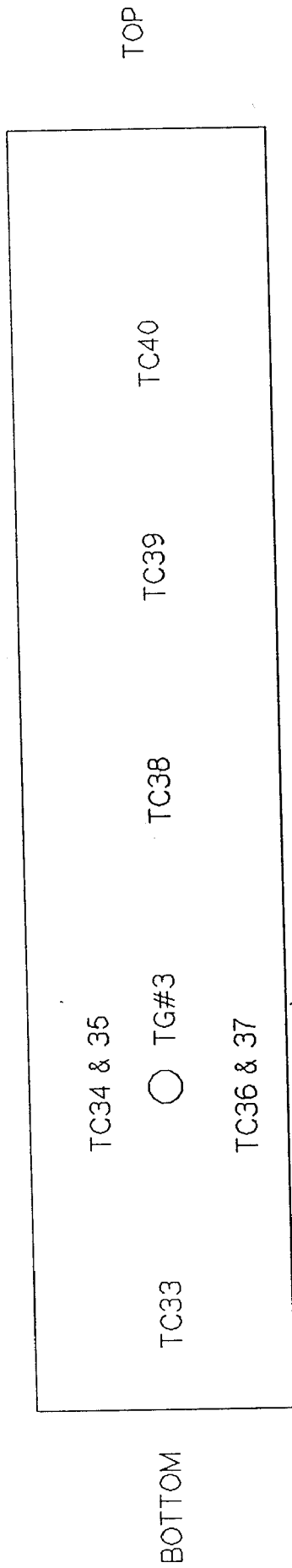


FIGURE 1: SMALL STAINLESS STEEL
CYLINDRICAL CALORIMETER



STAINLESS PLATE

TC57 & 58

NOTE: ALL TC'S ARE ON BACK SIDE EXCEPT 36,37,44, & 45
57 & 58 ARE FLAME TC'S, AT LEVEL OF TRANSPIRATION GAGES

MILD STEEL PLATE

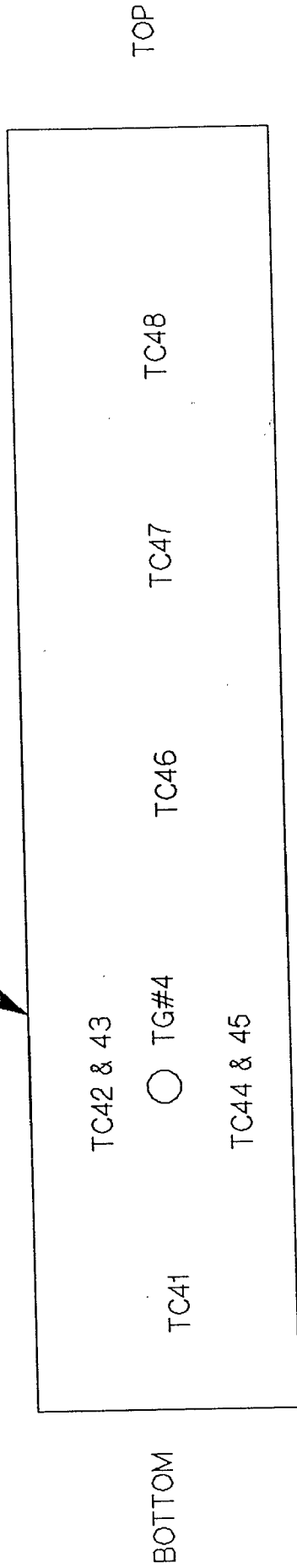


FIGURE 2, FRONT VIEW OF PLATE CALORIMETER

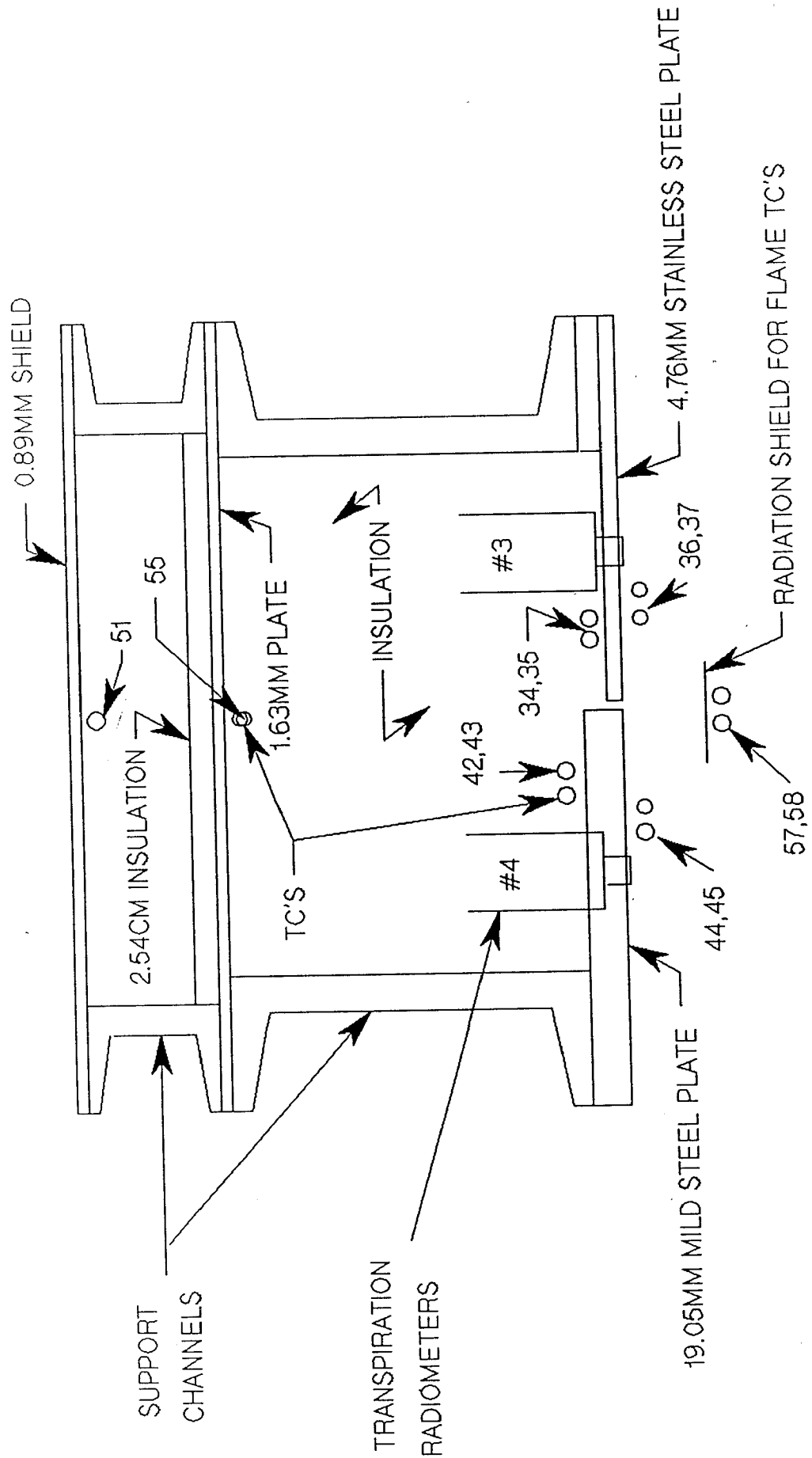


FIGURE 3, SECTION THROUGH PLATE CALORIMETER

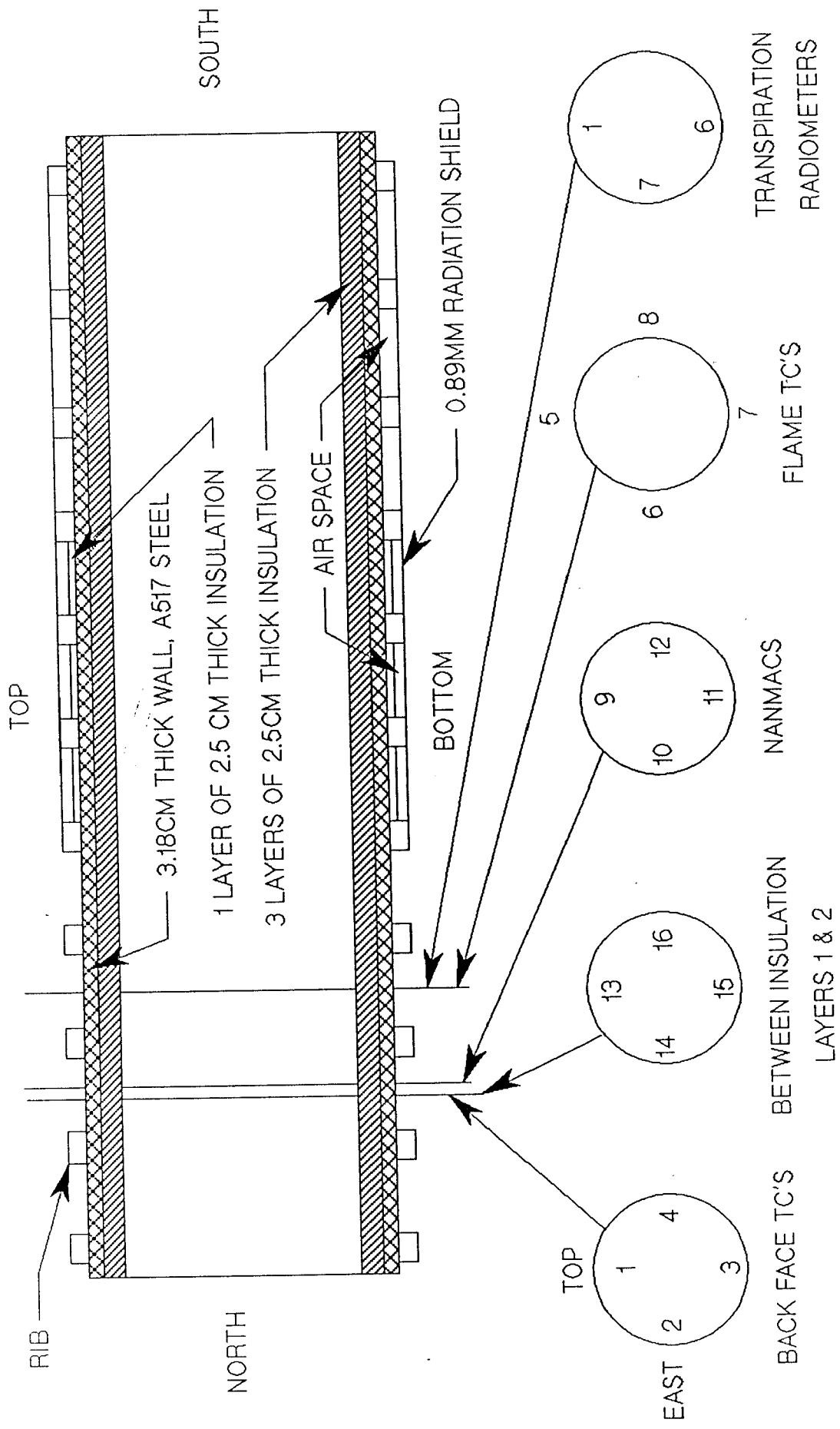


FIGURE 4, SIDE VIEW OF 1.4M DIA. CALORIMETER

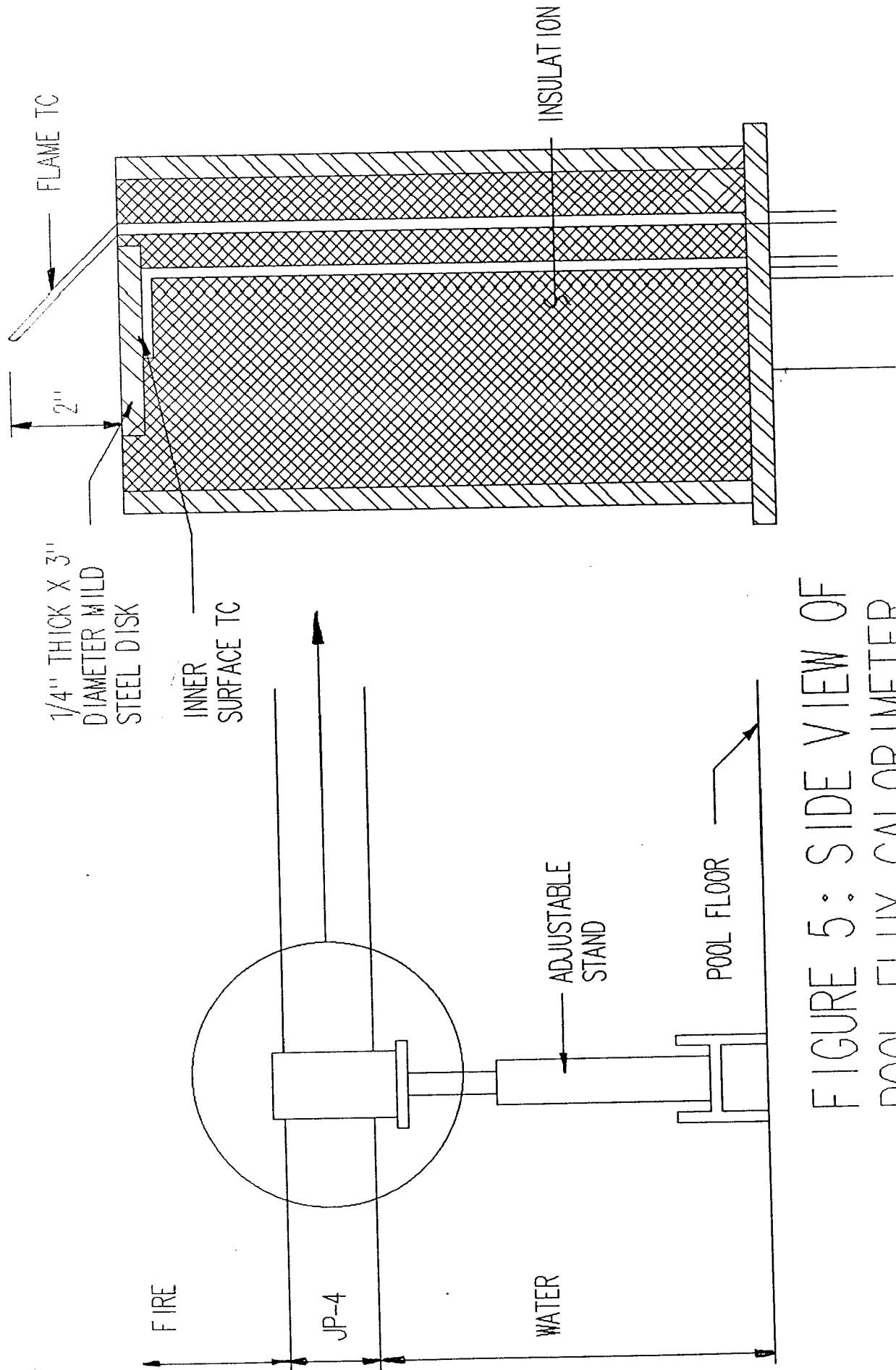


FIGURE 5: SIDE VIEW OF
 POOL FLUX CALORIMETER

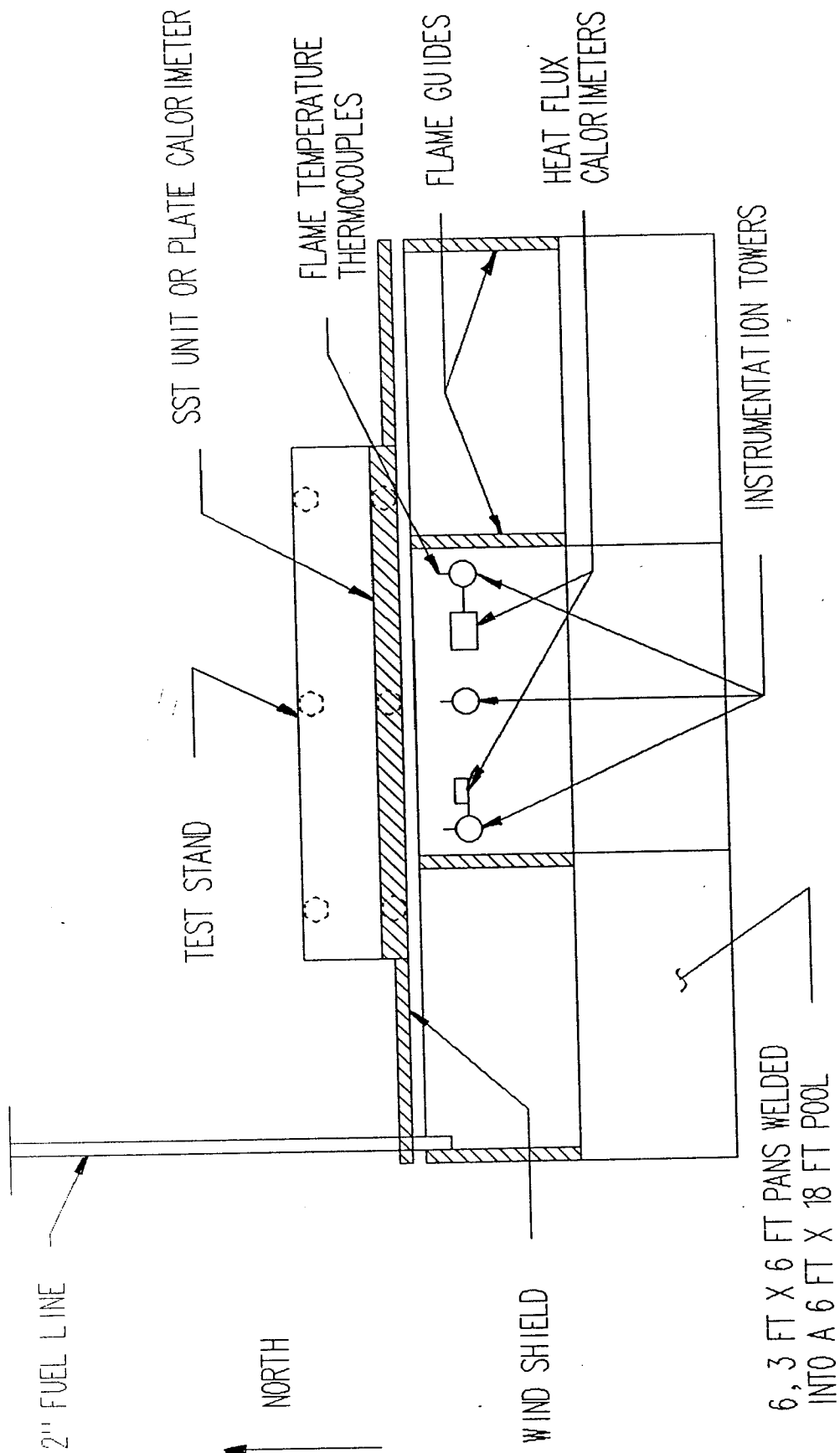


FIGURE 6: 1.8 M X 5.5 M
 POOL LAYOUT FOR SST TESTS

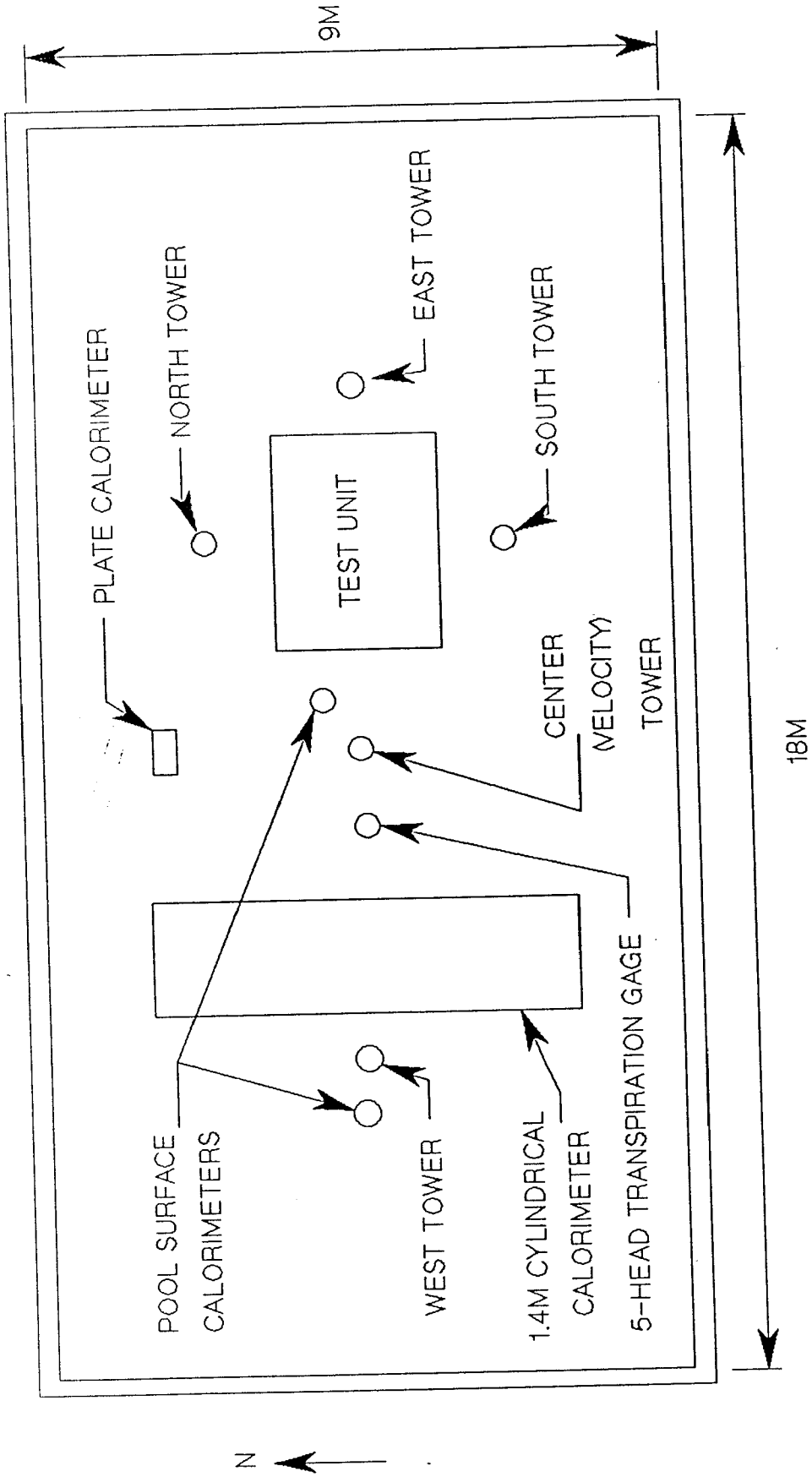


FIGURE 7: 9 M X 18 M POOL LAYOUT

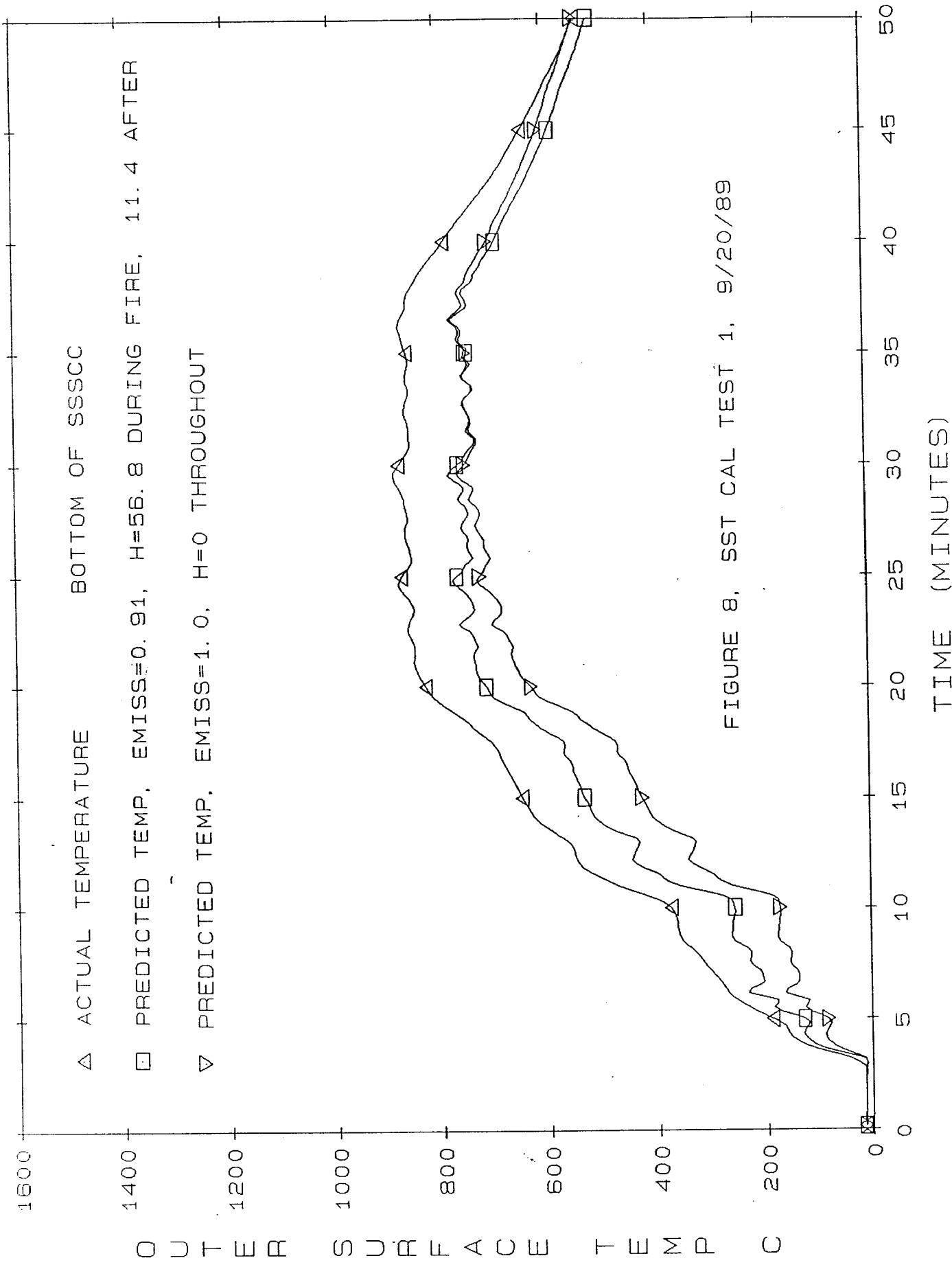


FIGURE 8, SST CAL TEST 1, 9/20/89

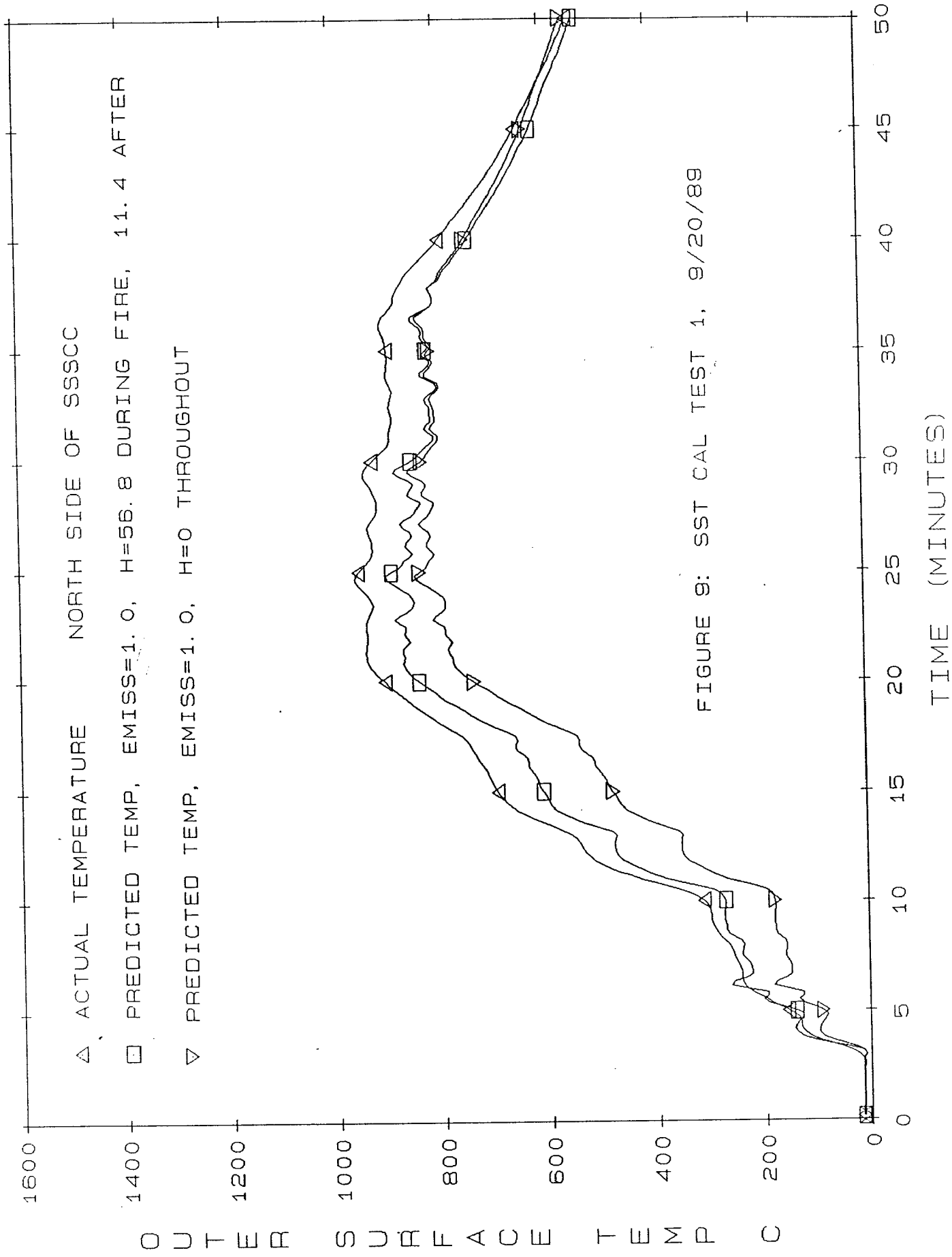


FIGURE 9: SST CAL TEST 1, 9/20/89

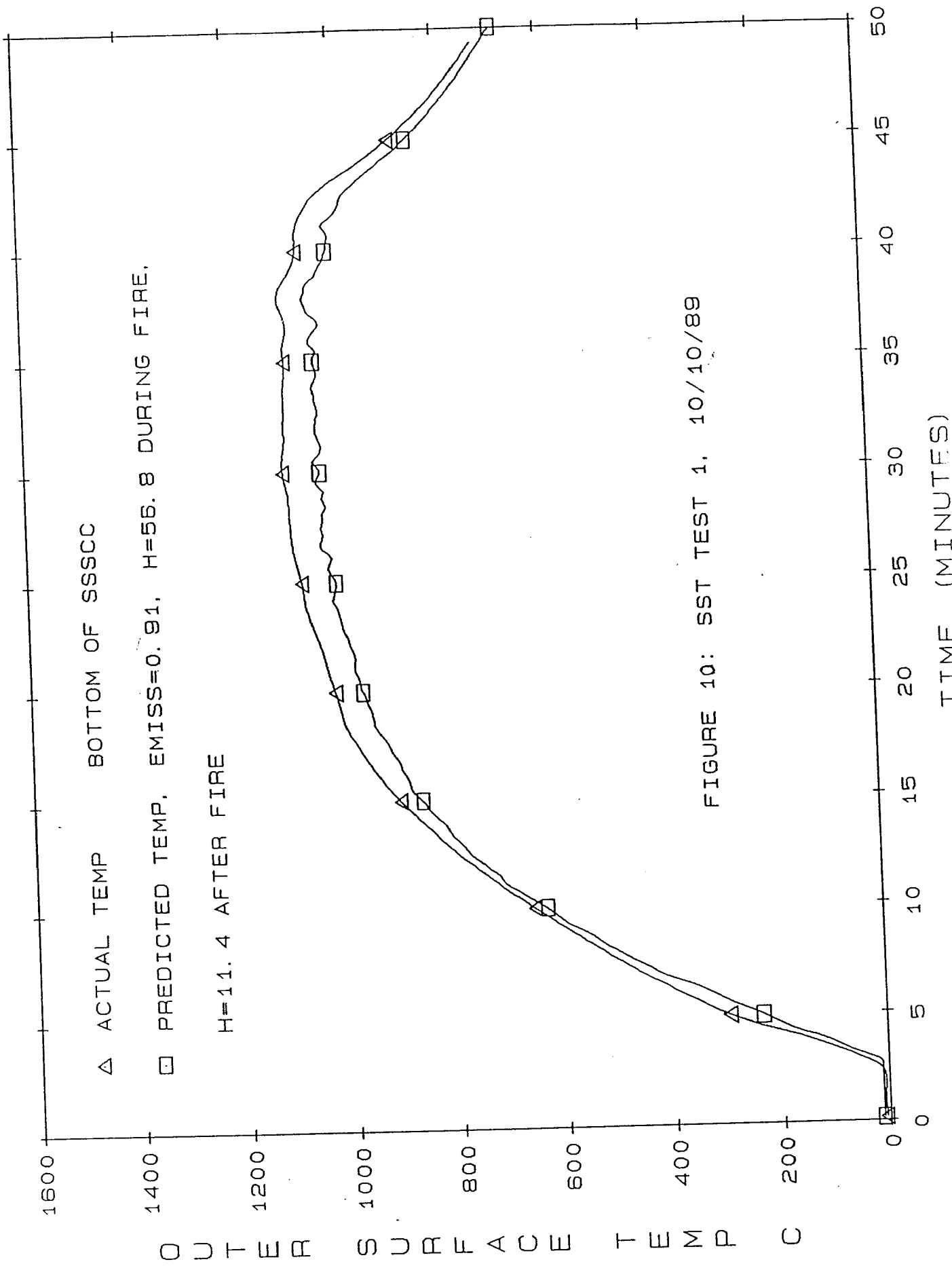


FIGURE 10: SST TEST 1, 10/10/89

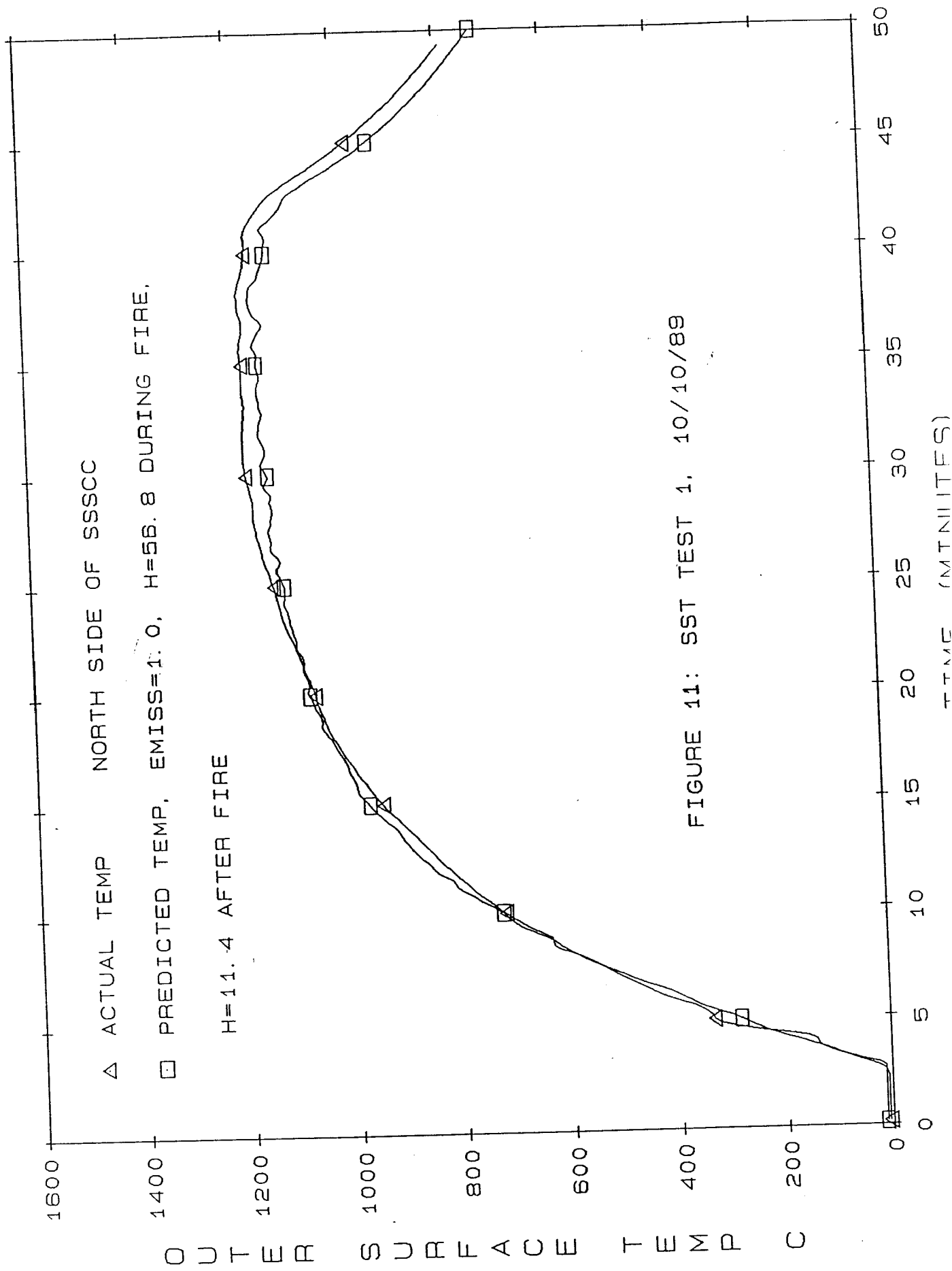


FIGURE 11: SST TEST 1, 10/10/89

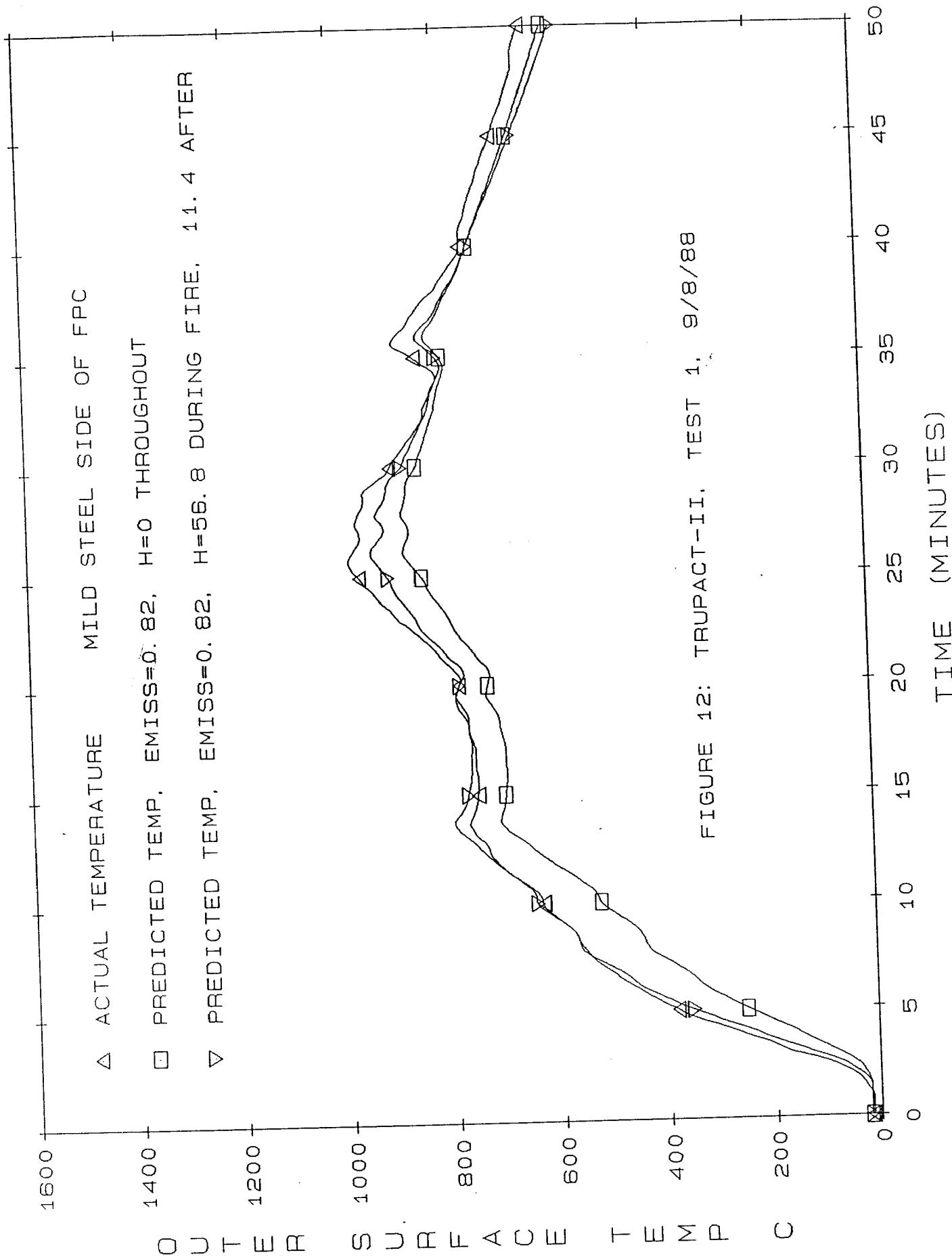


FIGURE 12: TRUPACT-II, TEST 1, 9/8/88